Automated Catheter Navigation with Electromagnetic Image Guidance

Herman A. Jaeger, Pietro Nardelli, Conor O' Shea, Josef Tugwell, Kashif A. Khan, Timothy Power, Michael O' Shea, Marcus P. Kennedy, and Pádraig Cantillon-Murphy

***Abstract*—This paper describes a novel method of controlling an endoscopic catheter using an automated catheter tensioning system with the objective of providing clinicians with improved manipulation capabilities within the patient. Catheters are used in many clinical procedures to provide access to the cardiopulmonary system. Control of such catheters is performed manually by the clinicians using a handle, typically actuating a single or opposing set of pull-wires. Such catheters are generally actuated in a single plane, requiring the clinician to rotate the catheter handle to navigate the system. The automation system described here allows closed-loop control of a custom bronchial catheter in tandem with an electromagnetic tracking of the catheter tip and image guidance using 3D Slicer. An electromechanical drive train applies tension to four pull-wires to steer the catheter tip, with the applied force constantly monitored though force sensing load-cells. The applied tension is controlled through a PC connected joystick. An electromagnetic sensor embedded in the catheter tip enables constant real-time position tracking while a working channel provides a route for endoscopic instruments. The system is demonstrated and tested in both a breathing lung model and a preclinical animal study. Navigation to predefined targets in the subject's airways using the joystick while using virtual image guidance and electromagnetic tracking was demonstrated. Average targeting times were 24 seconds and 10 seconds respectively for the breathing lung and live animal studies. This paper presents the first reported remote controlled bronchial working channel catheter utilising electromagnetic tracking and has many implications for future development in endoscopic and catheter based procedures.**

***Index Terms*—bronchoscopy, electromagnetic navigation, automation.**

I. Introduction

IMAGE guidance is becoming increasingly common in the fields of surgery and minimally invasive procedures [1], [2]. Image guided surgery (IGS) techniques allow the clinician to visualise the target of interest within a patient before and during the procedure. Guided surgeries and procedures have traditionally been performed directly by the surgeon through the use of intra-operative and pre-operative imaging modalities. Recent work shows the merging of image guidance techniques with assistive robotics [3], [4]. Assistive robotics can provide the clinician with increased accuracy, stability and scale of motion during surgery [5] while being comparable to traditional means in terms of procedure success and patient safety [6]. The majority of robotic surgeries today are performed for delicate urologic and gastroenterologic cases using automated laparoscopic systems such as the da Vinci Surgical System (*Intuitive Surgical Inc., USA*). Flexible robotic instruments have a potential advantage over laparoscopic instruments as they have the ability to conform to the natural curvatures present in the human body. Current research is focused on the development of continuum or 'snake-arm' robots [7], [8] to provide greater access to a patient's gastrointestinal tract. The Sensei Robotic System (*Hansen Medical Inc.*) is an example of a commercially available continuum catheter robot for vascular procedures with its first patients treated in 2010.

Fig. 1: (a) Olympus model 1T160 bronchoscope used in this work (b) Sensei X1 catheter system (*Hansen Medical Inc.*)

This paper describes the development of a novel endoscopic system with a particular focus on the area of image guided robot-assisted bronchoscopy. Image-guided bronchoscopy is a well documented procedure with studies showing its efficacy and safety in patients [9]–[11]. Virtual navigation and robotic assistance are the next steps currently being analysed in terms of feasibility and safety [12]. Three primary endobronchial methods are currently used by clinicians to navigate the airway: Traditional bronchoscopy, Endobronchial Ultrasound (EBUS) and Electromagnetic Navigation Bronchoscopy (ENB). Traditional bronchoscopy requires inserting a rigid or flexible scope into the airways of the patient where navigation is performed using optical fibre or a camera located at the distal tip. EBUS is an image-guided modality that complements traditional bronchoscopy by providing real-time ultrasonic imaging of the airway. Linear ultrasound probes can assist the clinician by providing detailed imaging of regions behind the airway wall. Guided biopsy of lymph nodes and masses not visible by the bronchoscope camera can be achieved in this manner. Radial ultrasound probes are used

This work is supported by the Irish Health Research Board and Science Foundation Ireland grant 15/TIDA/2846

A. Jaeger, P. Nardelli, C. O' Shea, J. Tugwell, T. Power, M. O' Shea and P. Cantillon-Murphy are with the School of Engineering, University College Cork, Cork, Ireland. Kashif Al Khan and Marcus Kennedy are with Cork University Hospital, Cork, Ireland.

for the localisation of distal tumours as they can reach deep into the bronchial tree to provide imaging of peripheral lung tissue [13]. ENB is a virtual guidance modality as it does not provide real-time imaging of the airway. Preoperative patient imaging is processed instead to form a 3-dimensional map of the airway network. This map is used with live position data from an electromagnetic tracking system to provide an accurate estimation of the current location within the airway. The SuperDimension Navigation System (*Medtronic, USA*) and Veran SPiNView [14] are examples of existing ENB systems which provide accurate image guidance but do not enhance or automate the control of tools at the target location.

In this work, a new assisted method of navigating a multi-purpose catheter is proposed. The method incorporates a custom tendon-driven catheter design with embedded electromagnetic sensor controlled with an electromechanical drive-train. The system allows the clinician to manipulate the catheter through a computer interfaced joystick. The system has been used successfully in-vivo to navigate and biopsy phantom nodules in the peripheral airways of a porcine subject. In this paper we present the mechanical system used to control the deflection of the catheter. The deflection properties of the catheter were examined to estimate the maximum force/deflection characteristic for each pull-wire tendon. The system was demonstrated in navigating the airways of a porcine subject through to the outer bronchi of the lung.

II. Background

Bronchoscopy is a common procedure to inspect the airways of a patient for the diagnosis/treatment of pulmonary disease. Clinicians use a bronchoscope to navigate the bronchi of the lung and are available in rigid and flexible varieties (Fig. 1). Flexible scopes allow increased manoeuvrability as they can conform to curvatures of the airway. Integrated optics can provide clinicians with a view of the airway through an eyepiece or video display equipment. The bronchoscope's working channel allows insertion of endoscopic instruments for biopsy and resection of tissues. Scope diameters range between 5-9mm depending on technical features and clinical application. Narrow airways whose diameters measure less than the scope diameter cannot be directly accessed and require advanced imaging methods to guide endoscopic tools toward regions of interest.

Image guidance techniques allow clinicians to navigate endoscopic tools beyond the line of sight of the endoscope. Fluoroscopy provides the clinician with real-time imaging [15] at the cost of exposing the patient to radiation. Electromagnetic navigation bronchoscopy (ENB) is a relatively new and increasingly popular technique that acts as a radiation-free alternative to fluoroscopy. ENB provides the clinician with information regarding endoscope and instrument position within a patient [16]. Commercially available systems include the SuperDimension Navigation System (*Medtronic, USA*), which use a tracked probe to place a nitinol or polymer sheath at the area of the lung to be investigated. While initially effective, multiple instrument insertions increase the risk of the sheath deviating from the target location, as the sheath tip is no longer tracked once the probe is removed. The Veran SPiNView Thoracic Navigation System (*Veran Medical, USA*) system improves on this by offering tip-tracked instruments to provide each endoscopic tool with a dedicated tracking sensor. While the system potentially increases position accuracy, distal tip manipulation is restricted to 180°deflections in a single plane and requires the use of proprietary tracked instruments.

The catheter design described in paper uses an electromagnetic navigation system developed in University College Cork [17] to verify successful targeting of phantom tumour models during *ex-vivo* and *in-vivo* experiments. The tracking system emitter board consists of eight planar transmitter coils (Fig. 2). The solver is implemented in Matlab and utilises the popular Levenberg-Marquardt (LM) algorithm [18] [19] with the trust region method [20]. An error function for the ith coil is shown in (1), where κ_i is the a calibration constant. The equation calculates the difference between the measured magnetic flux values and those calculated from the system model. For a single sensor due a single transmitter coil i the error between the measurement and model can be written as:

$$E_i = |\Phi^i_{meas}(r,\phi,\theta) - \kappa_i \Phi^i_{calc}(r,\phi,\theta)| \tag{1}$$

The algorithm resolves the position of the sensor in spherical coordinates (r,ϕ,θ) through minimisation of the cost function of the form:

$$F = \sum_{i=1}^{8} (E_i)^2 \tag{2}$$

The system has previously been evaluated in a breathing lung model with positional errors within 1.5mm [21]. The catheter described in this paper contains a commercially available 5 degree-of-freedom sensor compatible with the tracking system.

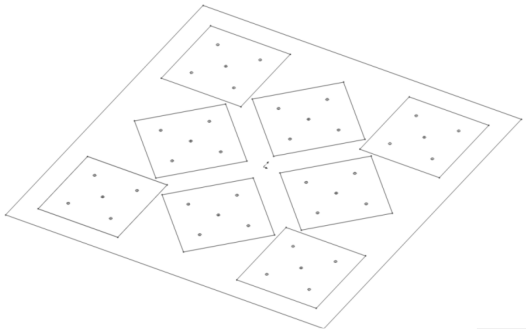

Fig. 2: Eight planar coils that comprise the tracking system emitter board.

III. Methods and Materials

This section describes the construction of the primary components of the catheter system. The catheter's design and construction will be initially be discussed. The accompanying control system and tracking software will then be described. A diagram highlighting these system components can be viewed in Fig. 4.

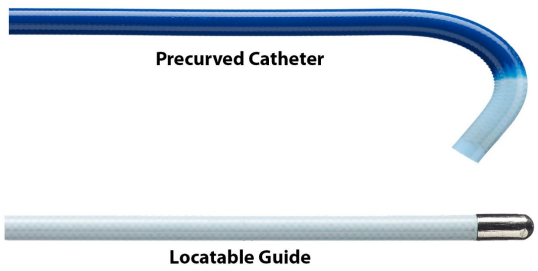

Fig. 3: Pre-curved Edge catheter and locatable sensor guide of the SuperDimension Navigation System (*Medtronic, Ireland*) The locatable guide is inserted though the catheter channel and must be removed prior to instrument use.

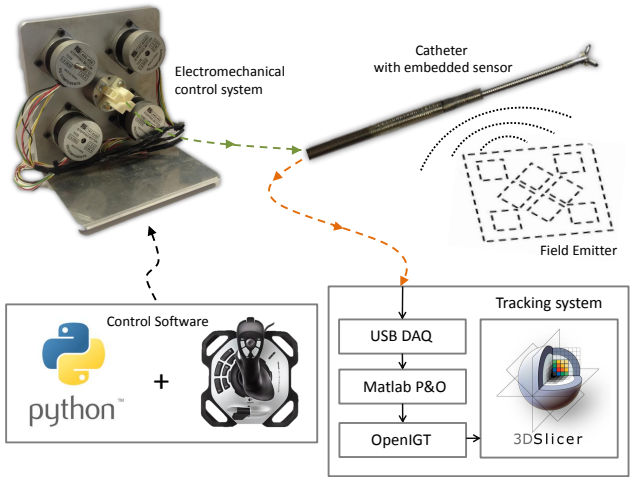

Fig. 4: Diagram of the catheter automation system. The catheter tip is manipulated by an electromechanical tensioning system connected to a control station. An attached joystick accepts and processes the clinician's input to steer the catheter tip in the desired direction. The tracking system is comprised of a USB data acquisition unit and solving algorithm to provide the clinician with a visualisation of the catheter tip 3D Slicer through the OpenIGTLink API.

A. Catheter Design

This work features a steerable catheter with outer diameter 2.6mm with a working channel diameter of 1.5mm for endoscopic instruments. The catheter is 105cm in length and incorporates a 5 degree-of-freedom electromagnetic sensor at the distal tip as shown in Fig. 5. The catheter tip tracking has been successfully tested with our electromagnetic navigation system [17]. The catheter can be steered by manipulating the four pull-wires connected to the distal tip. Varying the tension in adjacent pairs of pull-wires allows the catheter to be deflected in any direction. The catheter tip can be deflected in all directions up to 90° [22].

B. Mechanical Design

A control system was developed to allow the tension of the catheter pull-wires to be adjusted. The system consists of a rigid base housing four stepper motors (Fig 7(a)). The

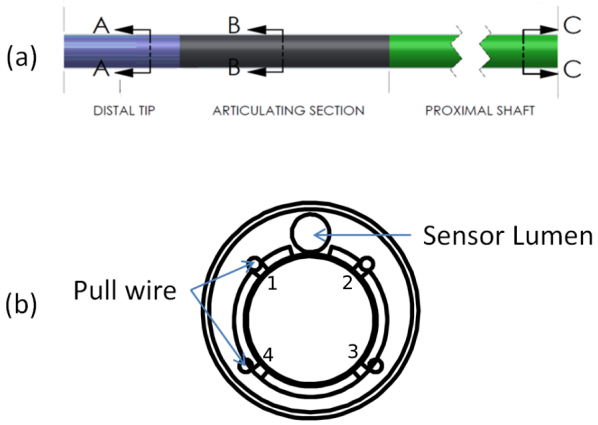

Fig. 5: (a) Catheter design with working channel. The distal tip (blue) houses the 5-DOF electromagnetic sensor used with the tracking system. (b) Cross section of distal tip showing four pull wires and sensor lumen.

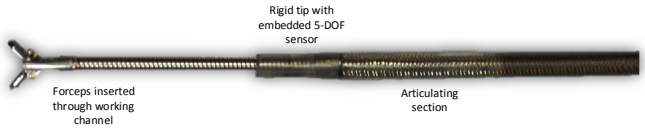

Fig. 6: Photograph of catheter with 1.2mm forceps inserted through the working channel.

stepper motors are configured for full-stepping and rotate 1.8 degree per step. Each motor is powered using a dedicated stepper motor integrated circuit connected to a microcontroller. The rotary motion of the stepper motors is translated to a linear motion using a belt and lead-screw. A lead-screw thread pitch of 1mm results in a linear resolution of 0.005mm. This configuration reduces the torque load on the stepper motors and provides an accurate method of manipulating the pull-wires of the catheter.

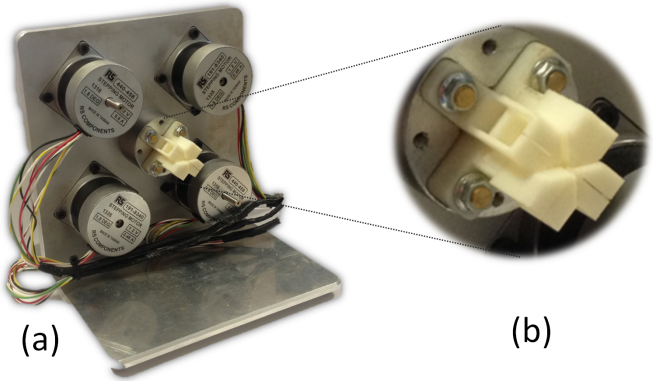

Fig. 7: (a) Electromechanical tensioning system. (b) Force sensing linear actuators for tensioning the catheter pull-wires.

Each linear train connects to one of the catheter pull-wires though a coupling method shown in Fig. 7(b). This mechanism provides access to the catheter's working channel and electromagnetic sensor. The instrument port was design with

a smooth bend and gradual taper to easily guide instruments into the working channel.

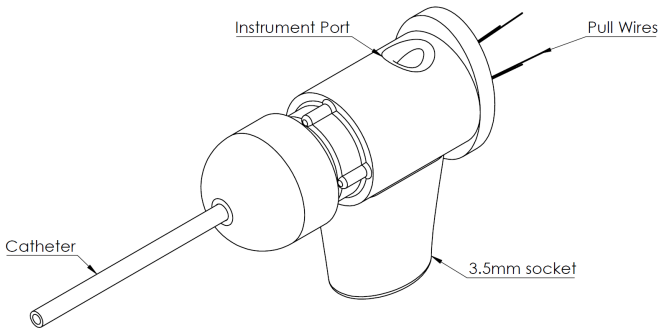

Fig. 8: Coupling design for automated catheter. The proximal end of the catheter is bonded to the proximal cap. The pull wires and sensor wire are fed through the main assembly after which the proximal cap is secured.

C. Driving Electronics

The tension control system runs on a single Teensy 3.1 microcontroller *(pjrc.com, Portland, Oregon, USA)* running at 96MHz. The catheter pull-wires are tensioned using two sets of opposing stepper motors. Each stepper motor was driven using an A3967 driver IC *(Allegro MicroSystems, Worcester, Massachusetts USA)*. The microcontroller controls the motor speed and monitors the pull-wire tensions. The tension in each pull-wire is sensed using a loadcell *(FSS1500NSB, Honeywell)*. The output of each loadcell was amplified using using an instrumentation amplifier *(INA122, Texas Instruments)* and measured using an analog to digital converter (ADS1015, Texas Instruments). A joystick *(Extreme 3D Pro, Logitech)* connected to a computer was used as the control input to the system by providing axis. A serial connection between the joystick and the controller was established though a Python script. A system update rate of 40Hz was empirically chosen to ensure a sufficient response time.

IV. Catheter Evaluation

The mechanical coupling load cells acquire tension data directly from the pull-wires of the catheter. The force required to achieve a desired tip deflection was measured using this approach. This data was used for predicting the deflection of the catheter tip. Tip deflection measurements were gathered for a range of forces applied individually to each pull-wire. A known force was applied to each pull-wire under test while ensuring the remaining wires were slackened. Deflection angles were measured relative to the catheter body using a protractor. Each wire was tested three times to ensure repeatability of the deflections. The resulting plots of deflection versus applied force are shown in Fig. 10.

The sigmoidal characteristic of each plot suggests there is hysteresis in the deflection of the tip. This non-linearity is due to the material composition of the catheter and cannot be avoided. For the purpose of this work, a first order approximation for relating the force to tip deflection was assumed. The data gathered from this experiment is used for a simple feedback control scheme.

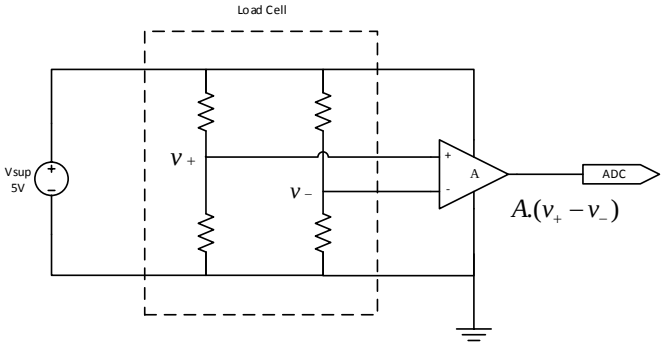

Fig. 9: Amplifier circuit for a single loadcell. The cell is composed of a piezoresistive bridge whose differential output is proportional to the applied force. The differential output of each loadcell is conditioned by an instrumentation amplifier such that the ADC can operate at full scale range

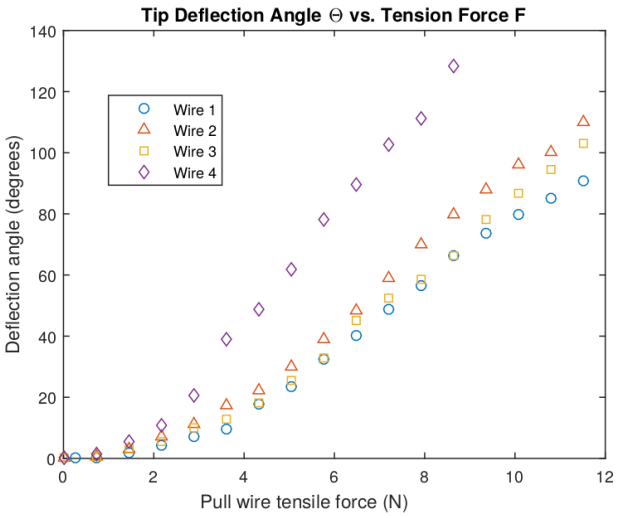

Fig. 10: Deflection curves for each pull-wire tendon in the catheter. Pull-wire #4 experienced noticeably increased deflection sensitivity compared to the other tendons.

TABLE I: Standard deviation of the deflection measurements for each tested pull-wire. Each plot displays

Wire No.	Standard deviation σ (N)
1	0.0291
2	0.0369
3	0.0438
4	0.0273

V. Threshold Control

A simple feedback controller was designed to perform deflections of the catheter tip according to the user's input from

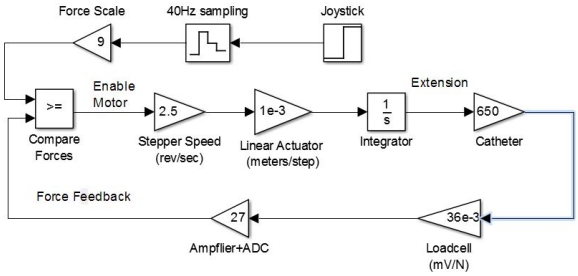

Fig. 11: Simplified block diagram of the simulated control scheme used for a single catheter pull-wire actuator. Joystick axis data is sampled at 40Hz and scaled appropriately. The scaling factor was chosen based on Fig. 10 where approximately 9N of force is required for 90°deflection. The catheter was approximated by a spring constant of 650N per meter calculated by applying a fixed displacement to a single pull-wire and measuring the resultant tension.

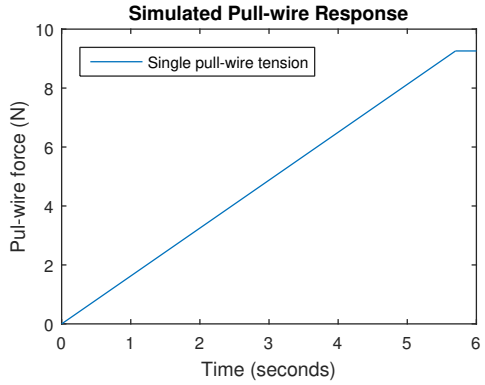

Fig. 12: Simulated response of a single pull-wire to a step change in required tension from 0-9N (90°deflection). Simulation predicts approximately 5.5 seconds to reach maximum deflection.

the computer connected joystick. The controller was designed to safely deflect and control the catheter tip within a testing environment. Catheter tension was assumed linear with pull-wire displacement and is represented by a spring constant for the purposes of simulation. This approximation was sufficient to allow for safe catheter operation and preventing over-tension on the pull-wires. A simplified block diagram of the control scheme is shown in Fig. 11.

The joystick axes are represented floating point vectors $[x, y]$ where $|x|, |y| < 1.0$. Each iteration of the algorithm acquires the sign and magnitude of the joystick axes. The axes correspond to opposing pair of actuators on the tensioning system, where the sign of each axis determines which of the pair engage. The appropriate actuators engage until the tension setpoint is reached. The tension produces a bending moment at the catheter tip to yield a deflection. Disengaged actuators automatically return to a pre-defined reset position to ensure opposing wire pairs do not get tensioned simultaneously. Simultaneous loading of opposing wires to the tip of the catheter, resulting in tip buckling and potential catheter damage.

VI. Preclinical Studies

A. Ex-vivo Experiment

Ex-vivo testing was carried out using the electromagnetic tracking system in conjunction with a breathing lung model shown in Fig. 13. The model consists of a vacuum chamber capable of inflating a set of preserved pig lungs. CT scans of the pig lungs acquired and segmented before the procedure and used to provide the user with real-time position feedback regarding the catheter tip position in the 3D Slicer environment. The purpose of this experiment was to verify the catheters functionality when used through a bronchoscope channel in a real airway and prepare for an in-vivo study. Radio-opaque phantom tumours [23] were placed in known locations in the periphery airways of the lung and provided the user with targets for the purpose of the test. Target size is a key variable in determining the likelihood of a successful biopsy as a forceps is more likely to sample a larger target. The contrast-infused tripe segments were chosen to measure 5mm to match typical small lesion sizes [24]. Peripheral nodule locations in Fig. 13 were chosen in order to simulate different biopsy scenarios.

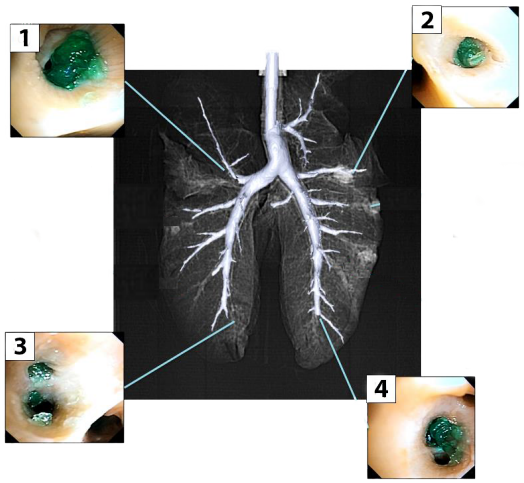

Fig. 13: Phantom tumour model locations in ex-vivo experiment. Targets 1 & 2 are located in the upper left and right lobes. These locations tested the catheter's ability to steer and navigate bifurcations. Targets 3 and 4 are located distally and tested the catheter's diameter and tracking system accuracy.

TABLE II: Time required in seconds to reach phantom tumour fiducial markers during ex-vivo study.

Fiducial No.	Time to target (seconds)
1	30
2	44
3	18
4	24
Mean time to target	29

Registration of the CT scans to the electromagnetic position data was carried out using a landmark registration based on Horn's method [25]. Four points from the reference frame of the CT scan were recorded along with their corresponding

locations in the EM tracking systems reference frame. The transformation between the EM tracker frame and the CT scan frame was then calculated and used during the procedure for updating location of the catheter tip in 3DSlicer.

B. In-vivo Experiment

In this section we describe the preclinical animal study and operation of the catheter automation system.

1) Procedure Setup: The animal was subject to CT scan visualisation with a GE 64 slice Discovery VCT scanner. CT scan parameters were 0.625mm slice thickness, 0.625mm slice separation and tube current of 60mA at 120 kV and standard kernel reconstruction. The CT image was segmented using the Airway Segmentation and Centreline Extraction modules in 3D Slicer [26].

2) Phantom Placement: Phantom tumours were used as fiducial markers for testing the system based on a tumour model recipe [23]. Seven separate tripe samples were endoluminally advanced through bronchoscope and endoscopic forceps, two in the upper right lobe (fiducials 1 & 3), one in the middle right lobe (fiducials 4), one in the upper left lobe (fiducial 2), one in the middle left lobe (fiducial 5) and two further co-located in the lower left lobe (fiducials 6 & 7). CT fluoroscopy was used to confirm placement position. Following the placement of tumour model markers, a second CT with identical scan parameters to the first scan was undertaken. This facilitated visualisation of the endoluminal tumour models within the airways and enabled segmentation on the 3D Slicer platform. Segmentation of the CT image was repeated using 3D Slicer to visualise the airways and tumour models using the same segmentation and reconstruction approach as described previously.

3) System Setup: The subject CT scan and segmentation was achieved using the bronchoscopy module [26]. The process took 4 minutes on a Dell Precision M4800 with i7 Intel quad-core processor operating at 3.6 GHz. A 10 cm cushion was placed between the emitter board and operating table *(Medstone Elite from Arcoma AB, Vxj, Sweden)* during tracking to limit tracking position errors due to table interference. A system was undertaken before scanning using reported protocols [17] with 49 points sampled within the operating environment. A set of predetermined landmarks points was used to calculate a registration matrix between the tracking system and segmented model using the same method as in the *ex-vivo* study [25].

4) Fiducial targeting: Tumour models were individually identified by the visual inspection of the segmented CT scan in 3D Slicer and seven independent tumour model targets were identified in both lungs. These were marked with manually placed virtual fiducial markers in 3D Slicer. The virtual bronchoscopy module in 3D Slicer was used to create virtual navigation pathways in advance of physical endoscopic navigation. A virtual pathway was successfully created in each target. Automated navigation and biopsy was attempted for 7 fiducial points. The connected joystick (Logitech Extreme 3D Pro) was used for catheter manipulation to the tumour target following positioning of the bronchoscope approximately 3 cm from the target. In each case, the tumour target was successfully navigated using joystick steering control. Once the navigated catheter was at the tumour target, biopsy was achieved with pulmonary biopsy forceps (1.5 mm Olympus endobronchial GuideSheath forceps K-202) inserted through the central lumen of the automated catheter. Withdrawal and visual inspection of the forceps post-biopsy confirmed successful targeting of the tumour target in each case.

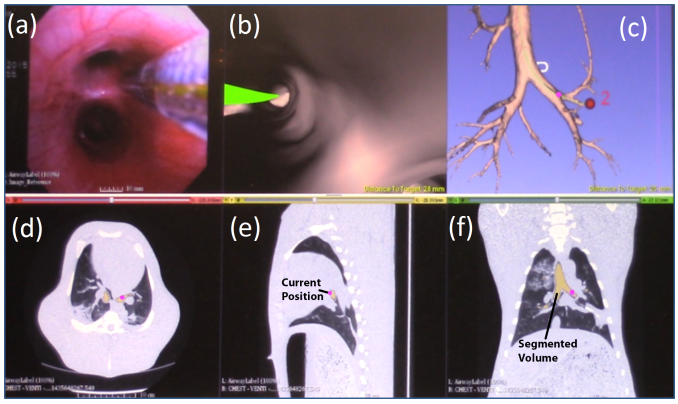

Fig. 14: Screenshot of 3DSlicer mid-procedure. (a) View from bronchoscope camera feed showing the automated catheter within the airway. (b) Virtual camera view showing a first person perspective of the airway relative to the catheter tip. The green line shows the planned route towards the target fiducial. (c) Zoomed-out model of the lung model showing target fiducial marker. (d)-(f) Coronal, sagittal and axial views of the original CT scans. The catheter location is shown as a purple dot in views (c)-(f). The CT slices change dynamically to show the current position of the catheter. Yellow areas represent a portion of the segmented airway volume (c) in the context of the current slice.

TABLE III: Time required in seconds to reach the phantom tumour fiducial targets during animal study.

Fiducial No.	Time to target (seconds)
1	18
2	14
3	10
4	8
5	6
6	7
7	5
Mean time to target	9.71

VII. Discussion

In this paper, we have demonstrated a novel endoscopic catheter design combining electromagnetic tracking and automation technologies. The automated catheter is successfully demonstrated *in vivo* in a preclinical study and is capable of navigating to multiple targets in the porcine subject's airway. Targeting times show an average targeting times of 29 seconds and 9.7 seconds for the breathing lung and and live animal studies respectively. The most challenging targets for the

catheter were those located in the upper lobes of the lung indicated by fiducials 1 & 2 in both studies. Navigation to these locations required significant curvature of the catheter tip and careful deflection of the joystick. In contrast, live study fiducial markers 6 & 7 were promptly targeted as they were located in the lower left of the lung and required relatively little deflection of the catheter tip.

Larger targeting times were experienced during the ex-vivo study. These navigation time differences may be a combination of learner effect and lung deformation. The *ex-vivo* study took place prior to the live animal trial, resulting in the clinician gaining experience in using the catheter system. The *in-vivo* targeting times could reflect this experience. Lung deformation could also play a key role in the differing times. The ex-vivo study used preserved pig lungs in a negative pressure chamber. The lungs were simply supported by a firm cushion within the chamber. Preserved lung tissue is soft, spongy and easily deforms due to breathing action and gravity in the absence of the supporting chest structure present in live subjects. As such, the lungs can never be reseated in precisely the same position and orientation as when the CT scan was originally obtained. This results in an inherent error between the actual airway and the generated virtual bronchial tree. This mismatch caused navigational errors particularly in the most distal, deformable regions of the lung. Similar tracking errors were caused due to breathing motion of the lungs. Generally preoperative CT scans are taken at full inspiration in order to maximise the airway volume , leading to a higher quality segmentation. This single scan does not take into account the dynamics of the lung during normal breathing action. Compensation techniques for this periodic error due to motion typically utilise a time domain approach to model the airway movement [27].

A number of limitations presented themselves during the *in-vivo* study. Most notably was the length constraint set by the catheter. The open-channel catheter in this paper was designed with a working length of 105cm to facilitate use with endoscopic tools of working length 110cm, giving 5cm of instrument headroom beyond distal tip of the catheter. The proximal portion of the catheter was directly coupled to the tensioning system (Fig. 7-8). The tensioning system was placed on an instrument table beside the clinician during the procedure. The distance from the system to the working channel of the bronchoscope resulted in the catheter having a reduced operating reach. This was particularly noticeable in the clinical setting where insertion of the catheter though the bronchoscope working channel became cumbersome at times for the testing clinician. Future work will see the development extension for the catheter to allow greater flexibility and operator freedom in the clinical setting while maintaining compatibility with commercially available endoscopic tools.

An important limitation of the study are tumour models and how they were created in the pig. The tumour models were placed distally using a standard bronchoscope. These models cannot be fully representative of peripheral tumours since they were placed with standard bronchoscopy techniques. The reach of the scope becomes an important limitation even though every effort was made to place the models at the most distal locations in the outer airway. Hence the models in this study should be viewed only as approximations to peripheral tumours arising in a real case. The electromagnetic navigation system used in this work could not have been used to place the models as the tracking system's efficacy with the catheter was the subject of the study. Future studies may see tumour models placed using real-time CT guided transthoracic needles to overcome this limitation.

In some cases the airway branches where a tumour target resides may not be segmented by 3DSlicer. This occurs due to the segmentation process relying on the quality of the CT scan. Variables including radiation dosage, patient movement and inspiration volume contribute to the quality of the resulting CT scan. In the event that a distal nodule's tree location get truncated, the software will generate a guide path which extrapolates the bronchial tree path to the target nodule [28]. This path is only an approximation and does not fully represent the missing tree, but serves as an adequate alternative for navigation purposes when CT quality is compromised.

Evaluation and control of the tensioning system was discussed in Section IV The deflection characteristics of the catheter were analysed by individually tensioning the pull-wires and recording both the tension forces and tip deflection angles. The threshold based control scheme developed around this data was sufficient for the purposes of testing the catheter design, but suffered from slow response times and occasional inconsistencies in resulting deflection angles. Fig.10 shows the non-linear deflection characteristics present in the design the catheter. The catheter in this work is a complex mechanical system formed with materials of varying elasticities, particularly at the flexible distal tip. The eccentric placement of the pull-wires in the wall of the catheter ()Fig. 5(b)) also result in tip deflection angles that are dependant on the overall curvature of main catheter body. In order to improve the accuracy and responsiveness of the tip deflection, a detailed mechanical model of the catheter needs to be developed that embodies pull-wire forces, displacement and tip deflection angles. Work in this area has been pursued for converting a desired catheter configuration to a set of catheter pull-wire displacements [29], [30].

VIII. Conclusion

This paper presents the first reported remote controlled, electromagnetically tracked catheter with a working channel and has many implications for future development in endoscopic and catheter based procedures. The work in this paper focused on combining existing electromagnetic navigation and automation technologies into endoscopic catheter design. We have applied the technology in a pre-clinical setting through bronchoscopy and have shown that automation techniques have the potential to assist in targeting lung lesions. The catheter assisted in the successful biopsy of multiple tumour targets by combining constant position tracking, automated tip steering and uninterrupted instrument use within the airway. This technology has other potential applications in ear, nose and throat (ENT) procedures and colonoscopy where radiological imaging techniques are not feasible. Future work on the automation system will involve refining the system design

to include a more responsive user interface that is fit for use in a clinical setting.

ACKNOWLEDGMENT

This work is supported by the Irish Health Research Board health research award POR/2012/31, the Irish Research Council Postgraduate Scholarship Scheme 2012-2015, the Science Foundation Ireland Technology Innovation Development Award 15/TIDA/2846. The authors would like to acknowledge the support of Mr. Kieran McManamon, Mr. Vincent Mehigan and Mr. Krishnan Gopal at the Biological Services Unit and the Centre for Research in Vascular Biology at University College Cork in pre-clinical investigations.

REFERENCES

[1] K. Cleary and T. M. Peters, "Image-Guided Interventions: Technology Review and Clinical Applications," *Annual Review of Biomedical Engineering*, vol. 12, no. 1, pp. 119–142, 2010.

[2] T. M. Peters, "Image-guidance for surgical procedures." *Physics in medicine and biology*, vol. 51, no. 14, pp. R505–R540, 2006.

[3] A. Hughes-Hallett *et al.*, "Intraoperative ultrasound overlay in robot-assisted partial nephrectomy: First clinical experience," *European Urology*, vol. 65, no. 3, pp. 671–672, 2014.

[4] P. Gilling *et al.*, "Aquablation - Image Guided Robotically-Assisted Waterjet Ablation of the Prostate: Initial Clinical Experience," *BJU International*, pp. n/a–n/a, 2015.

[5] A. R. Lanfranco *et al.*, "Robotic Surgery," *Annals of Surgery*, vol. 239, no. 1, pp. 14–21, 2004.

[6] P. C. Giulianotti *et al.*, "Robot-assisted laparoscopic pancreatic surgery: Single-surgeon experience," *Surgical Endoscopy and Other Interventional Techniques*, vol. 24, no. 7, pp. 1646–1657, 2010.

[7] Z. Li *et al.*, "A Novel Tele-operated Flexible Robot Targeted for Minimally Invasive Robotic Surgery," *Engineering*, vol. 1, no. 1, pp. 73–78, 2015.

[8] K. Kume *et al.*, "Development of a novel endoscopic manipulation system: The Endoscopic Operation Robot ver3," *Endoscopy*, vol. 47, no. 9, pp. 815–819, 2015.

[9] S. A. Merritt *et al.*, "Image-guided bronchoscopy for peripheral lung lesions: A phantom study," *Chest*, vol. 134, no. 5, pp. 1017–1026, 2008.

[10] N. Shinagawa *et al.*, "Virtual bronchoscopic navigation system shortens the examination time-Feasibility study of virtual bronchoscopic navigation system," *Lung Cancer*, vol. 56, no. 2, pp. 201–206, may 2007.

[11] H. Asahina *et al.*, "Transbronchial biopsy using endobronchial ultrasonography with a guide sheath and virtual bronchoscopic navigation," *Chest*, vol. 128, no. 3, pp. 1761–1765, 2005.

[12] S. Christie, "Electro magnetic navigational bronchoscopy and robotic-assisted thoracic surgery," *AORN Journal*, vol. 99, no. 6, pp. 750–763, jun 2014.

[13] A. Chen *et al.*, "Radial probe endobronchial ultrasound for peripheral pulmonary lesions: A 5-year institutional experience," *Annals of the American Thoracic Society*, vol. 11, no. 4, pp. 578–582, 2014.

[14] Veran Medical Technologies Inc. USA, "SPiNView Thoracic Navigation System," 2015.

[15] K. Tsushima *et al.*, "Comparison of bronchoscopic diagnosis for peripheral pulmonary nodule under fluoroscopic guidance with CT guidance," *Respiratory Medicine*, vol. 100, no. 4, pp. 737–745, 2006.

[16] S. Leong *et al.*, "Electromagnetic navigation bronchoscopy: A descriptive analysis," *Journal of Thoracic Disease*, vol. 4, no. 2, pp. 173–185, 2012.

[17] K. O'Donoghue *et al.*, "Catheter position tracking system using planar magnetics and closed loop current control," *IEEE Transactions on Magnetics*, vol. 50, no. 7, 2014.

[18] A. Plotkin *et al.*, "Magnetic tracking of eye motion in small, fast-moving animals," *IEEE Transactions on Magnetics*, vol. 44, no. 11 PART 2, pp. 4492–4495, 2008.

[19] P. G. Seiler *et al.*, "A novel tracking technique for the continuous precise measurement of tumour positions in conformal radiotherapy." *Physics in medicine and biology*, vol. 45, no. 9, pp. N103—-10, 2000.

[20] F. V. Berghen, "Levenberg-Marquardt algorithms vs Trust Region algorithms," *Methods*, no. 1, pp. 3–6, 2004.

[21] K. O'Donoghue *et al.*, "Evaluation of a novel EM tracking system in a breathing lung model," in *The Hamlyn Symposium on Medical Robotics, London, United Kingdom*, 2014, pp. 4046–4049.

[22] A. Jaeger *et al.*, "The Cork Lung Project: Automated Catheter Navigation," 2015.

[23] C. O'Shea *et al.*, "Evaluation of Endoscopically Deployed Radiopaque Tumor Models in Bronchoscopy," *Journal of Bronchology & Interventional Pulmonology*, vol. 23, no. 2, pp. 112–122, 2016.

[24] M. K. Gould *et al.*, "Evaluation of individuals with pulmonary nodules: When is it lung cancer? Diagnosis and management of lung cancer, 3rd ed: American college of chest physicians evidence-based clinical practice guidelines," *Chest*, vol. 143, no. 5 SUPPL, pp. 93–120, 2013.

[25] B. K. P. Horn, "Closed-form solution of absolute orientation using unit quaternions," *Journal of the Optical Society of America A*, vol. 4, no. 4, p. 629, 1987.

[26] P. Nardelli *et al.*, "Optimizing parameters of an open-source airway segmentation algorithm using different CT images." *Biomedical engineering online*, vol. 14, no. 1, p. 62, 2015.

[27] I. Gergel *et al.*, "An electromagnetic navigation system for transbronchial interventions with a novel approach to respiratory motion compensation." *Medical physics*, vol. 38, no. 12, pp. 6742–53, 2011.

[28] P. Nardelli, "Open-source Virtual Bronchoscopy for Image Guided Navigation," Ph.D. dissertation, University College Cork, 2016.

[29] D. B. Camarillo *et al.*, "Mechanics modeling of tendon-driven continuum manipulators," *IEEE Transactions on Robotics*, vol. 24, no. 6, pp. 1262–1273, 2008.

[30] ——, "Task-Space Control of Continuum Manipulators with Coupled Tendon Drive," *Springer Tracts in Advanced Robotics*, vol. 54, no. 4, pp. 271–280, 2009.